

Radius and Structure Models of the first Super-Earth Planet

Diana Valencia¹

*Earth and Planetary Science Dept., Harvard University, 20 Oxford Street, Cambridge, MA,
02138*

`valencia@mail.geophysics.harvard.edu`

Dimitar D. Sasselov

Harvard-Smithsonian Center for Astrophysics, 60 Garden Street, Cambridge, MA, 02138

and

Richard J. O’Connell

*Earth and Planetary Science Dept., Harvard University, 20 Oxford Street, Cambridge, MA,
02138*

ABSTRACT

With improving methods and surveys, the young field of extrasolar planets has recently expanded into a qualitatively new domain - terrestrial (mostly rocky) planets. The first such planets were discovered during the past year, judging by their measured masses of less than 10 Earth-masses (M_{\oplus}) or Super-Earths. They are introducing a novel physical regime that has not been explored before as such planets do not exist in our Solar System. Their composition can be either completely terrestrial or harbour an extensive ocean (water and ices) above a rocky core. We model the structure and properties of the first Super-Earth (mass $\sim 7.5 M_{\oplus}$) discovered in 2005, illustrating the possibilities in composition and providing radius evaluations in view of future detection of similar planets by transits. We find that a threshold in radius exists for which larger values indicate that a Super-Earth most certainly has an extensive water content. In the case of GJ876d this threshold is at about 12000 km. Our results show that unique characterization of the bulk composition of Super-Earths will be possible in future transit studies.

Subject headings: planetary systems — planets and satellites: individual GJ876d
— Earth

¹corresponding author

1. Introduction

In the last 11 years more than 200 exoplanets have been discovered but only in the last year the minimum mass for detection has been pushed down to allow for terrestrial planets. The first extra-solar planet with a mass lower than $10 M_{\oplus}$, i.e. a Super-Earth, was discovered last year by Rivera et al. (2005) orbiting an M4V star named GJ876. Its estimated mass is $7.5 \pm 0.7 M_{\oplus}$ and it has an orbital period of 1.94 days. It is close to the host star and the surface temperature is calculated to range between 430 and 650 K (Rivera et al. 2005). The star is known to have two gas giant planets GJ876b,c in 30 and 61 day orbits (Marcy et al. 1998, 2001). Hence, the planetary system of star GJ876 has both an architecture and a planet - the Super-Earth, that are unfamiliar to our Solar System experience. Two other low mass planets have been discovered in this year: OGLE-2005-BLG-390Lb ($\sim 5 M_{\oplus}$ at 5 AU — (Beaulieu et al. 2006)) and HD69830b ($\sim 10 M_{\oplus}$ at 0.08 AU — Lovis et al. (2006)) exemplifying the variety in Super-Earths that will be discovered in the near future with missions like *Kepler*.

Calculating the internal structure of a Super-Earth can help us determine how different or similar to the Earth this planet might be. One of our goals is to provide mass-radius relations that will help characterize Super-Earths discovered by the transit method. We show in this study the tools we have to characterize Super-Earths and use GJ876d as an example of our model capabilities and limitations. We first describe the numerical method used to obtain density, pressure, and temperature profiles as a function of radius and refer the reader for more details to Valencia et al. (2006), where we provided the first theoretical grid of models for Super-Earth planets. To calculate the planet's radius and internal structure we need to make reasonable assumptions about its composition. It might be completely rocky or might have accumulated a substantial amount of ices depending on the material available during formation. We show the results and implications for different likely compositions for GJ876b as an example that can be replicated for any Super-Earth. Additionally, we explore the effects of tidal heating that might be present in short period orbits (like GJ876d) and nonzero eccentricities.

2. Model

2.1. Numerical method and Equations of State

We model the planet as being composed of distinct, homogeneous in composition, spherical shells. For a terrestrial planet these shells are: the mantle that is divided into lower

mantle and upper mantle, and the core that depending on the temperature structure of the planet might be divided into a liquid outer core and a solid inner core, as is the case for the Earth. The composition for the different layers is taken from the mineralogical composition known for the Earth (McDonough & Sun 1995). The upper mantle is composed of olivine (ol) and higher pressure forms of olivine (wadsleyite (wd) and ringwoodite (rw)); the lower mantle develops when rw transforms to perovskite (pv) and ferromagnesiowustite (fmw), with an additional shell at high pressures when pv transforms to post-perovskite (ppv). The solid inner core in the Earth is composed of Fe and small quantities of Ni, and the outer liquid core is composed of Fe and a light alloy (see figure 1). The candidates for this alloy are S, Si, O, C and H and to this day there is no consensus on which one(s) or the amount(s). We have used in this study a composition of pure Fe and $\text{Fe}_{0.8}(\text{FeS})_{0.2}$ to show the uncertainties in the radius of a planet from the lack of knowledge of the composition of the core.

For planets that harbour a substantial H_2O /ice content (ocean planets), there is an additional layer overlying the rocky interior (mantle and core), composed of two shells - water above high pressure phases of ice. In some cases pressure is not high enough (amount of H_2O is not large enough) to solidify water and the ice layer is absent (figure 1). The thickness of the water is determined by the intersection between the PT curve of the planet and the melting curve of ice. In the case of low surface temperature, the planet will have an additional shell above the water layer composed of ice I — the lightest form of H_2O and negative Clapeyron slope – as is the case for Jupiter’s satellites.

The numerical model solves the following differential equations for density ρ , gravity g , mass m and pressure P in each shell with a Runge-Kutta 4th order solver:

$$\frac{d\rho}{dr} = -\frac{\rho(r)g(r)}{\phi(r)} \quad (1)$$

$$\frac{dg}{dr} = 4\pi G\rho(r) - \frac{2Gm(r)}{r^3} \quad (2)$$

$$\frac{dm}{dr} = 4\pi r^2\rho(r) \quad (3)$$

$$\frac{dP}{dr} = -\rho(r)g(r) \quad (4)$$

where $\phi(r) = \frac{K_S(r)}{\rho(r)}$ is the seismic parameter that can be calculated with an equation of state (EOS) for K_S , the adiabatic bulk modulus; G is the gravitational constant and r is the radius.

The model integrates from the surface inwards with boundary conditions for P , T , ρ and total mass (M). It starts with a guess for the planet’s radius (R) that yields a surface gravity value and determines the structure to the last shell where there could be excess or deficit in mass depending whether the starting R is too small or too big respectively. The model then uses a bisect-newton approach to determine the radius that yields zero mass and zero gravity at the center of the planet (within 5 meters).

The EOS that we have implemented for all layers except the water layer is the Vinet EOS, because is the best analytical EOS for extrapolation (Hama & Suito 1996):

$$K_T(\rho, 300) = 3K_0 (x^{2/3} - x^{1/3}) \exp \left(\frac{3}{2}(K'_0 - 1) (1 - x^{-1/3}) \right) \quad (5)$$

where $x = \frac{\rho}{\rho_0}$, K_0 and K'_0 are the isothermal bulk modulus and its first derivative at a reference state — zero pressure and 300 Kelvin — and $K_S = K_T (1 + \alpha\gamma T)$, where α is the thermal expansion coefficient and the Gruneisen parameter $\gamma = \gamma_0 x^{-q}$ with $q = -\frac{\partial \ln \gamma}{\partial \ln \rho}$. Most high-pressure experiments fit their data to the 3rd order Birch-Murnaghan EOS (BM3) that is derived from a truncation of the linear expansion of the Helmholtz free energy with strain to the third order (Poirier 2000). The extrapolation of this EOS is highly uncertain since the fourth term in the expansion might not be smaller than the 3rd term in some cases. We use the values for K_0 and K'_0 obtained from the literature corresponding to the BM3 EOS to obtain $P(V)$ and refit the data to the Vinet EOS within a volume compression between 1 and 2/3. The general trend is that K_0 is smaller by a few GPa and K'_0 is larger by ~ 6 -8% in the Vinet fit. We used the Ranghine-Hugoniot EOS from Stewart & Ahrens (2005) within the water region.

To incorporate the effects of temperature in the EOS we added a thermal pressure term (due solely to deviations in temperature from 300K) for core and mantle regions that translates into a thermal bulk modulus correction. With R the universal gas constant, $\theta = \theta_0 \exp \left(\frac{\gamma_0 - \gamma}{q} \right)$ as the Debye temperature and n as the number of atoms in the unit cell, the thermal correction is expressed as:

$$K_T(\rho, T) = K_T(\rho, 300) + \Delta K_{th}(\rho, T) \quad (6)$$

$$\Delta K_{th} = 3nR\gamma\rho (f(T) - f(T_0)) \quad (7)$$

$$f(T) = (1 - q - 3\gamma) \frac{T^4}{\theta^3} \int_0^{\frac{\theta}{T}} \frac{\xi^3 d\xi}{\exp \xi - 1} + 3\theta\gamma \frac{1}{\exp(\theta/T) - 1} \quad (8)$$

For the icy region we incorporated the temperature effects in the density via the thermal

expansion coefficient:

$$\rho(P, T) = \rho(P, 300) \exp \left[\int_{300}^T \alpha(P, T') dT' \right] \quad (9)$$

$$\alpha(P, T) = (a_0 + a_1 T) \left(1 + \frac{K'_0}{K_0} P \right)^{-b} \quad (10)$$

where a_0 , a_1 and b are coefficients determined at zero pressure.

2.2. Thermal model

In order to incorporate the temperature effect in the EOS we need to have a model describing the temperature profile in the planet. We use the Earth as our starting point and parameterized convection theory to model the temperature regime of Super-Earths. The surface heat flow on Earth (44TW Pollack et al. (1993)) reflects the heat from radioactive sources in the mantle (some authors also place potassium in the core) and secular cooling from an initial hot state. If we account for the concentration of heat sources in the crust (generating about 5-12TW (Davies 2001; Vacquier 1991; Taylor & McLennan 1998), we take 8TW), and assume a bulk silicate concentration of uranium, potassium and thorium, radioactive heat in the mantle accounts for $\sim 58\%$ of the total heat flow. In Valencia et al. (2006) we reported scaling the heat flow with mass for Earth-like planets as a first attempt to scale radioactive heat sources and secular cooling together. Here we refine this scaling by separating the treatment of the two sources. If we assume that the material that makes Super-Earths is the same as the bulk material for the Earth, then the radioactive heat sources scale with mantle mass. Planets that have larger mantles will have higher heat flows. It is difficult to scale secular cooling for a Super-Earth because we do not know the role that mass plays in the evolution of a planet. With the scaling laws derived in Valencia et al. (2006) and parameterized convection, we have found (Valencia et al, *in prep*) that a massive planet is likely to convect in a plate tectonic regime similar to the Earth. Intuitively, the more massive the planet is, the higher the Rayleigh number that controls convection, the thinner the top boundary layer (lithosphere) and faster the convective velocities. This scenario might aid subduction of the lithosphere causing the onset of plate tectonics. Thus, we adopt that the evolution of a Super-Earth might be one that leads to the same proportion of secular cooling to radioactive heating as in the Earth. This is the first attempt to scale secular cooling with mass.

We define the Rayleigh number Ra (dimensionless parameter that controls convection) in terms of the heat flux (q_s):

$$Ra = \frac{\rho g \alpha q_s / k}{\kappa \eta} D^4 \quad (11)$$

where g , k , κ , η are the average gravity, conductivity, diffusivity and viscosity of the mantle. The thickness of the top boundary layer is

$$\delta = a \frac{D}{2} \left(\frac{Ra}{Ra_{crit}} \right)^{-1/4} \quad (12)$$

independent of the size of the mantle, where $Ra_{crit} \sim 1000$ is the critical Rayleigh number and a is a coefficient of order unity. We treat viscosity in two ways: i) isoviscous case and ii) a temperature dependent treatment $\eta(T) = \eta_0 (\frac{T}{T_0})^{-30}$ (see Valencia et al. (2006) for more details).

The planet modeled in this study has a convective core, mantle and ice/water layer where the temperature can be described as adiabatic:

$$\frac{dT(r)}{dr} = \frac{\rho(r)g(r)T(r)}{K_S(r)} \gamma(r) \quad (13)$$

All interfaces between the chemically distinct layers develop boundary layers that transfer heat conductively

$$\frac{dT}{dr} = -\frac{q}{k} \quad (14)$$

Their thickness depends strongly on the local viscosity. Owing to the low viscosity of the core and water we only model conductive boundary layers at the top and bottom of the mantle. The top boundary layer thickness is described in equation (12). In an isoviscous internally heated case, the bottom boundary layer of the mantle would vanish. Conversely in an isoviscous heated-from below case it would have the same thickness as the top one. Since we assume these planets are in a intermediate regime (same as Earth) the bottom boundary layer is taken to be half of the top one, and the heat flux reflects the heat coming out of the core.

Even though there are two critical assumptions in determining the temperature structure — the constant ratio between internal heating and secular cooling, and the thickness of the lower boundary layer in the mantle — the effects of temperature in the internal structure of a planet are small, particularly the effects in radius. The temperature profile is needed mostly to determine the location of the phase changes that determine the different regions in the planet. A temperature dependent viscosity increases the radius by ~ 20 km compared to the iso-viscous case showing that neither assumption is critical.

The numerical model iterates several times until convergence exists between the boundary layer thickness and the radius (i.e. surface heat flux) so that the temperature profile is determined self-consistently.

The numerical model needs as input the composition of the different regions as well as the proportion of ice mass fraction (IMF) and core mass fraction (CMF), and surface P and T. The output is: density, pressure, temperature, mass and gravity as a function of radius; the total radius and the location of the phase changes and composition boundaries. Table 1a shows the different values in composition used in this study. The composition assumes that the mantle minerals have 10% of iron and 90% magnesium in the mineral structures, except for post-perovskite phase that is believed to incorporate more Fe (Mao et al. 2004) where we adopt a 20% Fe by mol composition. Table 2 shows the values we used to determine the phase boundaries between the major silicate phase changes (ol to wd, rd to pv+fmw, pv to ppv), the phase boundary between water and ice is determined from a Krauss-Kennedy melting curve proposed by Stewart & Ahrens (2005). We calculate the melting point of iron by using a Lindeman equation (see Valencia et al. (2006) for details) only to test whether the core is in a solid or liquid phase but not to distinguish between different phases within the core (as is the case for the Earth). Only the Earth-like composition yields a planet hot enough to have a liquid core (see figure 3). A planet with more water content (IMF=40%) will have a smaller mantle for a given CMF and will be cooler (due to less radioactive heating) than a less water rich planet (IMF=20%). The strong dependency of the Gruneisen parameter with volume in the mantle (pv or ppv) (that determines the adiabatic gradient) prevents the temperature at the core-mantle boundary of being hot enough in planets with medium to small mantles (ocean planets with medium cores and rocky planets with large cores). The adiabatic gradient within the mantle remains small and the temperature increase within the mantle is not sufficient to allow for a liquid core (figure 3).

2.3. Composition cases for GJ876d

We consider a few basic scenarios for the composition of GJ876d that are representative but probably not exhaustive. They are (1) a simple Earth-like composition, a planet with a core that makes up 33% of the total mass, with a mantle that is 10% (by mol) iron enriched, and a lower mantle composed of 30% fmw and the rest pv. (2) an Earth-like, but with a very large core (mass fraction of 80%), (3) an ocean planet with a 20% by mass water/ice layer on top of a terrestrial (Earth-like) core, and (4) an ocean planet with a 40% water/ice layer. Our reasons for introducing the later three scenarios are: case (2) is analogous to Mercury - with its very close orbit, GJ876d might have similarly acquired a massive core

during its formation - this case is essentially a Super-Mercury (see Valencia et al. (2006) for details). Cases (3) and (4) are inspired by the possibility (Zhou et al. 2005) that GJ876d actually formed beyond the snow line in the protoplanetary disk of GJ876. The snow line in a disk is the distance from the star at which the local temperature and pressure in the midplane allow ices to exist during planet formation (Sasselov & Lecar 2000). In our Solar System the snow line was at about 2-3 AU, but GJ876 is a small $0.32 M_{\odot}$ star (Rivera et al. 2005). With its lower energy output and smaller size, GJ876 would define a snow line at ~ 0.25 AU in its passive disk at zero age. Beyond the snow line, ices (mostly H_2O) increase the solid fraction in the disk by a factor of ~ 4 , given the solar composition of the star. Therefore a Super-Earth forming in this region of the disk could acquire and retain water as a major fraction (20% or more) of its total mass. Differentiation will quickly produce an Earth-like core and interior overlaid by water ice (higher pressure ice phases such as VII and X) and a deep water ocean, similar to the ocean planets described by Leger et al. (2004). A more complicated issue is whether this water could evaporate during the lifetime (~ 6 Gyr) of the planet. A simple thermal escape estimate precludes that. It is possible to retain an icy/liquid layer over the age of this planetary system with a surface temperature of ~ 550 K provided the atmospheric pressure is large enough. Ice VII is stable at such temperature given pressures larger than a few GPa (Stewart & Ahrens 2005). Furthermore, the atmospheric partial pressure would have to exceed ~ 100 MPa to prevent the water layer from evaporating (Wagner & Pruss 2002). A non-thermal escape calculation is beyond the scope of this paper; it could prove very efficient in removing a lot of water from GJ876d, especially during the early evolution of the star.

Addressing the issue of bulk planet composition is central to our study. The case of GJ876 provides us with useful constraints. First, we know (Rivera et al. 2005) that the star has a composition very similar to the Sun and is of similar age. Second, there is evidence that the orbits of the GJ876 planets evolved shortly after planet formation by inward migration - the very close orbits of all 3 planets and the 1:2 mean-motion resonance state of the giant planets (Zhou et al. 2005)

3. Results

For the Earth-like composition case (lines with stars in top figure 2) perovskite transforms to post-perovskite at a radius of ~ 9800 km, so most of its mantle is actually composed of ppv+fmw. This brings attention to this relatively newly discovered phase present in the

lower-most mantle on Earth (only between 125 to 136 GPa) and the importance of determining with accuracy its behaviour at high pressures. If this planet had a pure Fe core, its radius would extend to 10800 km or $1.70 R_{\oplus}$ (Earth radius) and an additional 130 km ($1.71 R_{\oplus}$) if the core was composed of $\text{Fe}_{0.8}(\text{FeS})_{0.2}$. Despite the large differences in core density (300 kg/m^3) between the two core compositions, due to the different locations of the core-mantle boundary that satisfy the CMF, the radius differs by very little. This implies that the radius for planets with medium sized cores is a robust parameter.

The second scenario looks at the effect of having a larger CMF of 80% (see top figure 1) where we expect the composition of the core to have a larger effect. A planet that has a larger iron content presumable mostly in its core, can accomodate more of its mass in the central region and therefore have a smaller radius compared to an iron-poor planet. This type of planets (Super-Mercuries, Valencia et al. (2006)) exhibit comparatively large bulk densities as Mercury does in our Solar System. If GJ876d had a core of 80% by mass its radius would only be 9200 km (or $1.45 R_{\oplus}$) for pure Fe core and 9600 km (or $1.5 R_{\oplus}$) for a sulfur enriched core.

Next consider the possibility of this planet having a water/ice layer amounting to 20% and 40% of the total mass on top of a terrestrial core (bottom figure 2). Despite ice and water being highly compressible (bulk modulus is 1-2 orders of magnitude smaller respectively than for silicates), their densities at initial compression are low and the relation of the density gradient to density is quadratic. Consequently, a large amount of water makes the planet larger. If the Earth had a substantial amount of water the radius would extend to 7100 km ($1.11 R_{\oplus}$) for 20% water content and 7600 km ($1.19 R_{\oplus}$) for 40% water content. Figure 2 shows the density structure and figure 3 - the pressure-temperature structure for the different composition cases considered above. The ocean planets have a layer of water above a layer of denser ice due to the positive Clapeyron slope of ice VII (note the melting curve of ice VII in figure 3). Hemley et al. (1987) showed that ice transforms gradually from ice VII to ice X with pressure and proposed an EOS for the combined system. We have adopted those values for this calculation. Below the ice layer the pressure is $\sim 150 \text{ GPa}$, beyond the transition pressure between pv and ppv ($P=125 \text{ GPa}$ at $T=2750\text{K}$ Tsuchiya et al. (2004)), therefore the silicate mantle is made of ppv+fmw — perovskite and upper mantle silicate phases are absent. If GJ876d had a water/ice layer that accounted for 20% and a core that accounted for 33% of the total mass, the radius would be 11900 km (or $1.87 R_{\oplus}$). An additional 20% of water would extend the radius 550 km more (to $1.95 R_{\oplus}$). These radii are 11 and 15% larger respectively, compared to the Earth-like composition radius result. Such planets will be easier to detect when transiting their stars. Adding sulfur to the core would extend the radius of

both ocean planets by ~ 130 km. The radius results for all compositions are shown in Table 3.

In summary, the four bulk compositions produce differences in the Super-Earth mean densities and radii that are large enough - from 3% to 30% in radius, to be observationally measurable. For example, if GJ876d was transiting its star, MOST satellite photometry (Rowe et al. 2006) could achieve 3% precision in its radius, with uncertainty dominated by the stellar radius ($R = 0.32R_{\odot}$).

Our main result is that with a measurement of both mass and radius (even with a precision of 10%) we could certainly tell between an iron rich differentiated terrestrial planet ($R < 9600$ km) and a water rich (IMF > 20%) ocean planet ($R > 12000$ km). This is because there is a limited family of compositions that would fit both. To illustrate this point we have calculated the trade-off curve between the amount of ice (IMF) and core (CMF) that would satisfy $M = 7.5M_{\oplus}$ and $R = 11900$ km (see Figure 3). The maximum of amount ices this planet could harbour is $\sim 49\%$ with CMF = 51% and no mantle. The minimum could be zero if the planet had no core. This extreme case (no core) is so unlikely that a radius detection of 11900 km or more would necessarily mean that the planet has a water layer. Hence, knowledge on just the radius and mass of a planet – in combination with internal structure models — could yield valuable structural and compositional information on the planet and its formation environment.

4. Tidal heating effects

The Super-Earth’s extreme close proximity to its star GJ876 means that even small perturbations on its orbit might induce significant additional heating from tides and change its internal structure. We check this by a simple analysis, with a surface heat flux consisting of energy from radioactive heat sources, secular cooling and tidal heating. We add different amounts of tidal heating Q_{tidal} to the heat flow Q (see section 2.3) that translate in higher Rayleigh numbers and thinner lithospheres and calculate the thermal structure:

$$Q_{total} = Q + Q_{tidal} \quad (15)$$

For the calculation of the effects of internal heating we assume a temperature dependent viscosity. A simple analysis states that the energy dissipation rate produced by an eccentric orbit in a synchronous planet is (Murray & Dermott 1999)

$$\frac{dE}{dt} = \frac{63}{4} \frac{e^2 n}{\bar{\mu} Q_d} \left(\frac{R_p}{a} \right)^5 \frac{GM_{\star}^2}{a}$$

where G is the gravitational constant, M_\star is the mass of the star, a is the semimajor axis, n is the mean motion, $\tilde{\mu}$ is the ratio of elastic to gravitational forces, $\tilde{\mu} \approx (10^4 \text{km}/R_p)^2$, and Q_d is the specific dissipation parameter. In other words the energy available for tidal heating of the $7.5 M_\oplus$ Earth-composition planet GJ876d is

$$1.2 \times 10^{22} e^2 [W] \quad (16)$$

where $Q_d = 280$ as for the Earth (Ray et al. 2001). Figure 5 shows the effects of different values of dE/dt on the PT regime for this planet. In addition, figure 5 also shows the solidus for MgO, the lower mantle mineral with the lowest melting temperature. By increasing the amount of tidal heating the internal temperature rises and in some cases the lowermost mantle might be partially molten. Our calculations show that large increments in tidal heating cause small increments in internal temperature. Thus, in order to melt the lowermost mantle, the tidal heating needs to exceed $\sim 6.8 \times 10^{17} \text{W}$ for this $7.5 M_\oplus$ planet (or $\approx 10^{17} \text{W}/M_\oplus$), meaning 2500 times the heat flow without tidal heating. Even though the internal temperature is much higher than without tidal heating, the radius only increases by ~ 100 km. For planet GJ876d melting could commence for eccentricities above 0.008. While we do not yet know the dynamic environment of this planet very well, such eccentricities are not excluded (Rivera et al. 2005). We note that the newly discovered $\sim 10 M_\oplus$ Super-Earth HD69830b (Lovis et al. 2006) orbiting at 0.08 AU from a $0.86 M_\odot$ star is also in a 3-planet system and appears to have a non-zero $e = 0.10 \pm 0.04$. Hence its tidal heating could exceed $10^{17} \text{W}/M_\oplus$. HD69830b is expected to be mainly rocky (Lovis et al. 2006) and we estimate its radius at $1.84 R_\oplus$ (Valencia et al. 2006).

5. Uncertainties

The uncertainties in the model come from uncertainties in the EOS and the composition of the planet that needs to be known at high pressures and temperatures. Any phase change has to be known a priori in order to be incorporated in the model. Therefore when we extrapolate to high pressures it is possible that the material might change into a different phase that we can not account for without experimental evidence. If there are high-pressure phases unaccounted for in the model, the radius here obtained for different compositions would be an overestimate owing to the denser character of high-pressure minerals. Benoit et al. (1996) describes a transition of H_2O to ice XI at 300 GPa. GJ876d with IMF=40% reaches a maximum pressure of 350 GPa at the bottom of the ice shell. Therefore, the effects of ice XI would be to decrease the radius by a few tens of kilometers for this planet and more

for planets with larger masses and IMF.

The likely compositions chosen for GJ876d yield a central pressure between 2500 and 5000 GPa. Values that exceed any laboratory experiment up to date (Cohen et al. 2000). The extrapolation of EOS — Vinet and 3rd order Birch-Murnaghan — is yet to be tested at these pressures. Nevertheless, the uncertainty in composition is greater than errors in this extrapolation. The difference in radius from using the two different EOS is ~ 100 km, less than the difference due to the different compositions considered here. There are also uncertainties in the determination of the parameters in the EOS that translate into uncertainties in the internal structure. We considered two different data sets for the EOS of pure Fe (Uchida et al. 2001; Mao et al. 1990) and find that the difference in radius is only of ~ 65 km for the planet dominated by core composition.

Finally, the different treatments in viscosity (isoviscous vs. temperature dependent) only yield a difference in radius of ~ 20 km, though the temperature regime is different for the four compositions described herein. Our lack of knowledge on the temperature structure is offset by the small temperature effects in the total radius of the planet. This means that despite the uncertainties in the thermal model (viscosity assumptions and heat flow scaling assumptions) the radius is a robust parameter. Therefore we place an estimate on the error in radius of ~ 200 km due to the lack of knowledge associated with the EOS and in the thermal profile.

6. Conclusions and Discussion

In conclusion, the new surveys and improved detection techniques have opened up the study of a new class of objects, Super-Earths, that brings us closer to characterizing the exoplanets most similar to Earth. In particular, we can model the internal structure of the first discovered Super-Earth by looking at likely compositions. We find that the radius varies between ~ 9200 and 12500 km. If the orbital geometry allowed a transit follow up to GJ876d, the expected flux drop would be of $1.9 - 3.6 \times 10^{-3}$, large enough to be observed. If observed with a large-aperture telescope (Holman et al. 2005) or from space, e.g. with MOST (Rowe et al. 2006), a transiting planet like GJ876d would yield a radius determination with $\sim 3\%$ precision and one would be able to distinguish between all four scenarios/models presented by us here, especially between an iron rich differentiated and an ocean planet. Moreover, for a given mass there is a radius that delimits the boundary between ocean planets and terrestrial planets. If GJ876d radius was larger than 12000 km, it would indicate it is an ocean planet.

With the upcoming space mission *Kepler* that ability will improve, especially with expected advances in RV measurements (hence planet masses) for *Kepler's* fainter targets. Therefore, when radii measurements of terrestrial planets become available, we can put constraints on the bulk composition of a planet (given its mass) and begin to understand the conditions on distant terrestrial planets. A following article will treat this problem by showing in a simple manner the relation between radius, mass and composition.

7. Acknowledgements

We would like to thank the anonymous reviewer for his/her useful comments. This work was supported under grant NSF grant EAR-0440017. Diana Valencia acknowledges support from the Harvard Origins of Life Initiative.

REFERENCES

- Beaulieu, J. P., Bennett, D. P., Fouque, P., Williams, A., Dominik, M., Jorgensen, U. G., Kubas, D., Cassan, A., Coutures, C., Greenhill, J., Hill, K., Menzies, J., Sackett, P. D., Albrow, M., Brillant, S., Caldwell, J. A. R., Calitz, J. J., Cook, K. H., Corrales, E., Desort, M., Dieters, S., Dominis, D., Donatowicz, J., Hoffman, M., Kane, S., Marquette, J. B., Martin, R., Meintjes, P., Pollard, K., Sahu, K., Vinter, C., Wambsganss, J., Woller, K., Horne, K., Steele, I., Bramich, D., Burgdorf, M., Snodgrass, C., Bode, M., Udalski, A., Szymanski, M., Kubiak, M., Wieckowski, T., Pietrzynski, G., Soszynski, I., Szewczyk, O., Wyrzykowski, L., Paczynski, B., & Collaboration, T. M. 2006, Discovery of a Cool Planet of 5.5 Earth Masses Through Gravitational Microlensing
- Benoit, M., Bernasconi, M., Focher, P., & Parrinello, M. 1996, Phys. Rev. Lett., 76, 2934
- Cohen, R., O.Gulseren, & Hemley, R. J. 2000, Amer. Mineralogist, 85, 338
- Davies, G. 2001, Dynamic Earth: Plates, Plumes and Mantle Convection (Cambridge University Press), 458
- Dziewonski, A., & Anderson, D. 1981, Physics of the Earth and Planetary Interiors, 25, 297
- Fei, Y., Mao, H., & R.J., H. 1993, J. Chem. Phys, 99, 5369

Table 1. Compositional data

layer	composition	ρ_0 (kg/m ³)	K_0 (GPa)	K'_0	γ_0	q	θ_0	ref
<i>ocean</i>	H ₂ O	998.23	2.18	-	-	-	-	1
<i>shell</i>	ice VII+X	1463	2.308	4.532	1.2	1.	1470 ³	2,3
	...				$a_1=-4.2 \times 10^{-4}$	$a_2=1.56 \times 10^{-6}$	$b = 1.1$	2
<i>upper</i>	ol	3347.	126.8	4.274	0.99	2.1	809	4
<i>mantle</i>	wd+rw	3644.	174.5	4.274	1.20	2.0	908b	4
<i>lower</i>	pv+fmw	4152.	223.6	4.274	1.48	1.4	1070	4
<i>mantle</i>	ppv+fmw	4270.	233.6	4.524	1.68	2.2	1100	5
<i>core</i>	Fe	8300	160.2	5.82	1.36	0.91	998	6,7
	Fe _{0.8} (FeS) _{0.2}	7171	150.2	5.675	1.36	0.91	998	6,7

References. — Compositional data used in each shell of the model has been taken from different sources and refit to the Vinet EOS: (1) Stewart & Ahrens (2005) — Rankine-Hugoniot EOS (2) Hemley et al. (1987) (3) Fei et al. (1993) (4) Stixrude & Lithgow-Bertollini (2005) — A reuss average was performed according to a mixture of 10% Fe and 30% fmw for the bulk modulus. The thermodynamic parameters (γ_0 , q and θ_0) were taken from the most dominant phase in each shell. (5) Tsuchiya et al. (2004) – an increase in density was needed to account for 20% Fe in ppv according to $\partial \ln / \partial x = 0.3$ where x is the iron content (Mao et al. 2004). A Reuss average was then used with fmw. (6) Williams & Knittle (1997) — we also tried Uchida et al. (2001) parameters for density and bulk modulus and found a discrepancy in the radius of only 60 km for a composition of CMF=80%. (7) Uchida et al. (2001)

Table 2. Phase boundaries in silicate mantle

transition	boundary	
ol \rightarrow wd+rw	T=400P-4287	
rw \rightarrow pv+fmw	P=22.6	if T > 1750K
	T=13573-500P	if T \leq 1750K
pv+fmw \rightarrow ppv+fmw	T=133P-1392	

Note. — Table showing the different phase boundaries between the silicate mantle minerals used in this study. P is in GPa and T is in K.

Table 3. GJ875d radius

RADIUS	Fe	Fe _{0.8} (FeS) _{0.2}
Earth-like	10786 km	10914 km
Rocky CMF=80%	9228 km	9580 km
Ocean IMF=20%	11890 km	12014 km
Ocean IMF=40%	12448 km	12576 km

Note. — Radius results for the different four bulk compositions for a pure Fe core and a core with Fe and S. The only appreciable difference of 400 km happens in a core-dominated planet.

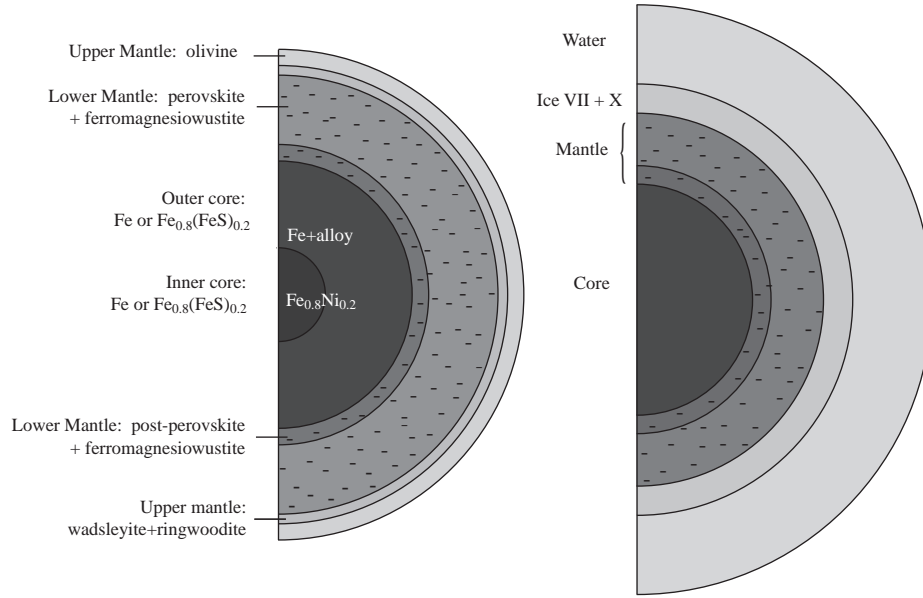


Fig. 1.— Schematic representation of the model. To calculate the internal structure of Super-Earths we assume a similar composition to the Earth’s: A dense core of pure Fe or $\text{Fe}_{0.8}(\text{FeS})_{0.2}$ as end member cases (the Earth has an outer core of Fe plus some unknown alloy and the solid inner core has Fe and Ni); a lower mantle composed of two silicate shells (ppv+fmw, pv+fmw); an upper mantle composed of two silicate shells (wd+rw, ol). The thickness of the shells will depend on the PT profile for the planet and the amount of mass in the core. An ocean planet - right - will have an additional water/ice layer above the rocky core.

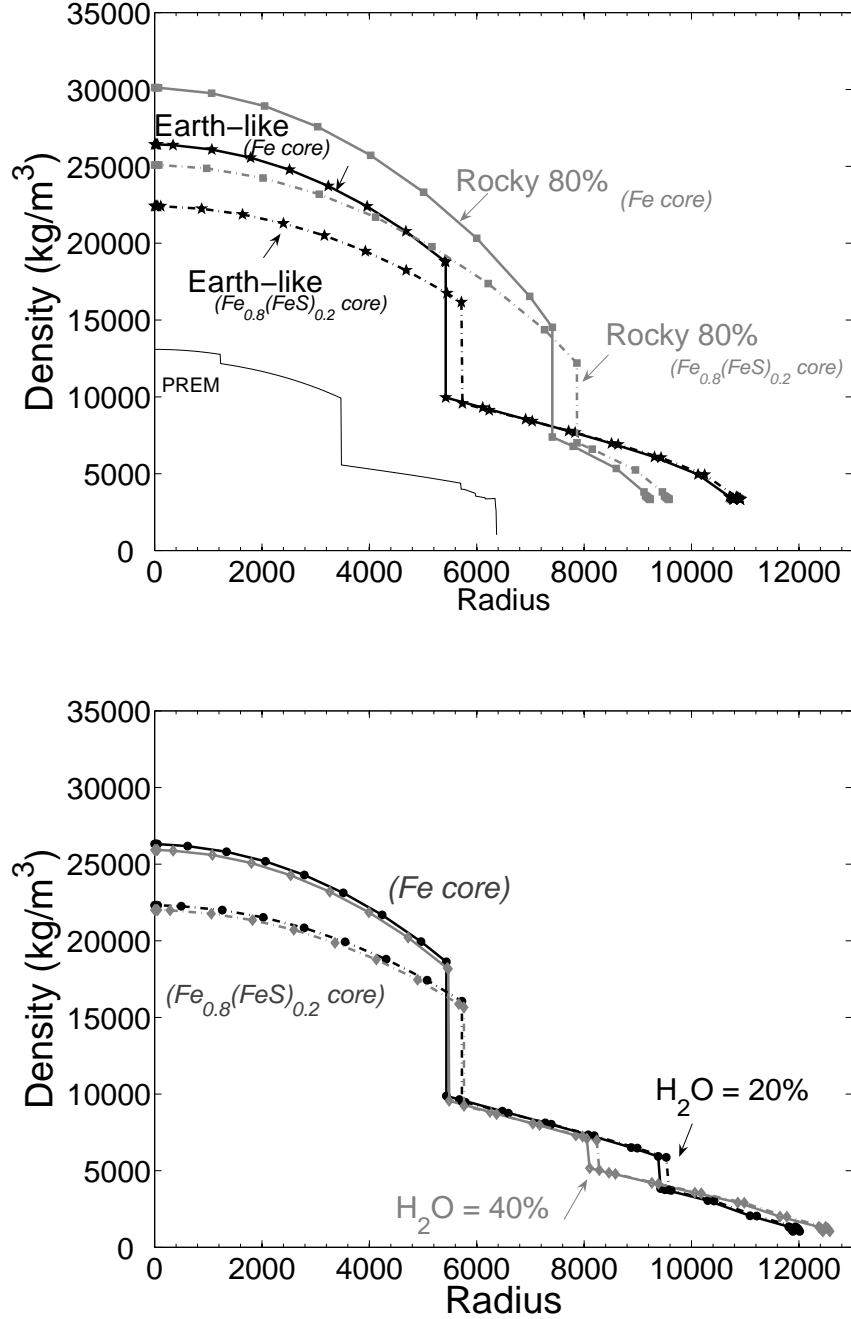


Fig. 2.— Internal Structure of exoplanet Gliese 876d: Density Profile. Four different compositions are illustrated. The surface is on the right and the centre of the planet is on the left. The solid lines show the cases for which the composition of the core is taken to be pure Fe. Dashed lines are for the case of $\text{Fe}_{0.2}(\text{FeS})_{0.8}$. Lines with stars shows the internal structure of GJ876d if the composition was Earth-like. Square symbols show the density profile if this planet had 80% of the mass in the core. Circles show the structure if this planet had formed outside the snow line and retained 20% of its mass as a water/ice layer. Diamonds shows the density structure if GJ876d had retained 40% of water/ice. A Preliminary Reference model for Earth (PREM – Dziewonski & Anderson (1981)) is shown for reference.

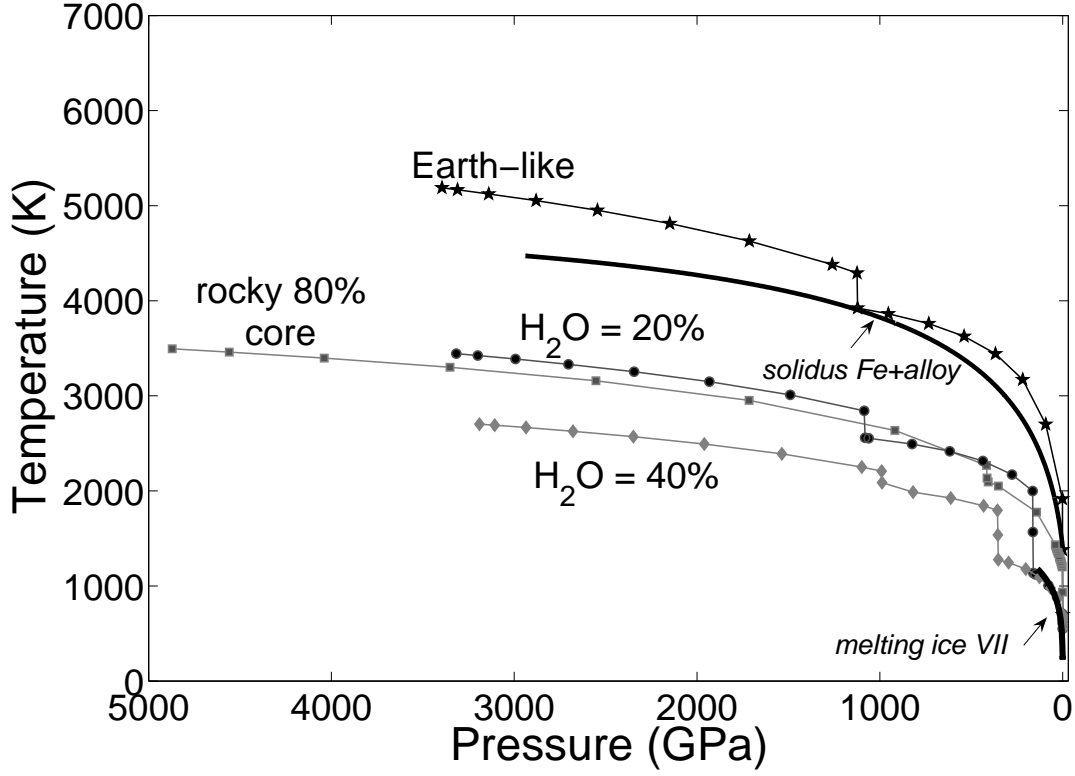


Fig. 3.— Internal Structure of exoplanet Gliese 876d: Pressure-Temperature Structure. The PT structure of GJ876d is illustrated considering the four compositions presented in this study and pure Fe in the core. The ocean-compositions cross the ice VII solidus at ~ 55 GPa which leaves means the water layer is 1200 km deep for both ocean planets (IMF=20% and IMF=40%).

- Hama, J., & Suito, K. 1996, *J. Phys. Condens. Matter*, 8, 67
- Hemley, R. J., Jephcoat, A. P., Mao, H. K., Zha, C. S., Finger, L. W., & Cox, D. E. 1987, *Nature*, 330, 737
- Holman, M. J., Winn, J. N., Stanek, K. Z., Torres, G., Sassellov, D. D., Allen, R. L., & Fraser, W. 2005, *ArXiv Astrophysics e-prints*
- Leger, A., Selsis, F., Guillot, C. S. T., Despois, D., Mawet, D., Ollivier, M., Labeque, A., Valette, C., B., F. B., Chazelas, & Lammer, H. 2004, *Icarus*, 169, 499
- Lovis, C., M.Mayor, Pepe, F., Alibert, Y., Benz, W., Bouchy, F., Correia, A. C. M., Laskar, J., Mordasini, C., Queloz, D., Santos, N. C., Udry, S., Bertaux, J., & Sivan, J. 2006, *Nature*, 441, 305
- Mao, H. K., Wu, Y., Chen, L. C., & Shu, J. F. 1990, *J. Geophys. Res.*, 95, 21737
- Mao, W. L., Shen, G., Prakapenka, V. B., Meng, Y., Campbell, A. J., Heinz, D. L., Shu, J., Hemley, R. J., & Mao, H.-k. 2004, *PNAS*, 101, 15867
- Marcy, G. W. R. B., Fischer, D., S.S.Vogt, Lissauer, J., & Rivera, E. 2001, *ApJ*, 556, 296
- Marcy, G. W. R. B., Vogt, S. S., Fischer, D., & Lissauer, J. 1998, *ApJ*, 505, L147
- McDonough, W., & Sun, S.-s. 1995, *Chem. Geol.*, 120, 223
- Murray, C. D., & Dermott, S. F. 1999, *Solar System Dynamics* (Cambridge University Press), 166–174
- Poirier, J. 2000, in *Introduction to the Physics of the Earth’s Interior* (Cambridge University Press), 63–109
- Pollack, H., Hurgter, S., & Johnson, R. 1993, *Rev. of Geoph.*, 31, 267
- Ray, R. D., Eanes, R., & Lemoine, F. G. 2001, *Geophys. J. Int*, 144, 471
- Rivera, E. J., Lissauer, J. J., Butler, R. P., Marcy, G., Vogt, S. S., Fischer, D. A., Brown, T. M., Laughlin, G., & Henry, G. W. 2005, *ApJ*, 634, 625
- Rowe, J. F., Matthews, J., Seager, S., Kuschnigand, R., Guenther, D., Moffat, A., Rucinski, S., Sassellov, D., & Weiss, G. W. W. 2006, *ApJ*
- Sassellov, D., & Lecar, M. 2000, *ApJ*, 528, 995
- Stewart, S. T., & Ahrens, T. J. 2005, *J. Geophys. Res.*, 110, 1

- Stixrude, L., & Lithgow-Bertollini, C. 2005, *Geophys. J. Int*, 161, INPRESS
- Taylor, S., & McLennan, S. M. 1998, *The continental Crust: Its composition and Evolution* (Blackwell)
- Tsuchiya, T., Jun, T., Kiochiro, U., & Renata, M., W. 2004, *Earth Planet. Sci. Lett.*, 224, 241
- Uchida, T., Wang, Y., Rivers, M. L., & Sutton, S. R. 2001, *J. Geophys. Res.*, 106, 21799
- Vacquier, V. 1991, *Geophys. J. Int*, 106, 199
- Valencia, D., O’Connell, R. J., & Sasselov, D. D. 2006, *Icarus*, 181, 545
- Wagner, W., & Pruss, A. 2002, *J. Phys. Chem. Ref. Data*, 31, 387, doi:10.1063/1.11461829
- Williams, Q., & Knittle, E. 1997, *Physics of the Earth Planetary Interiors*, 100, 49
- Zhou, J.-L., Aarseth, S. J., Lin, D. N. C., & Nagasawa, M. 2005, *ApJ*, 631, L85

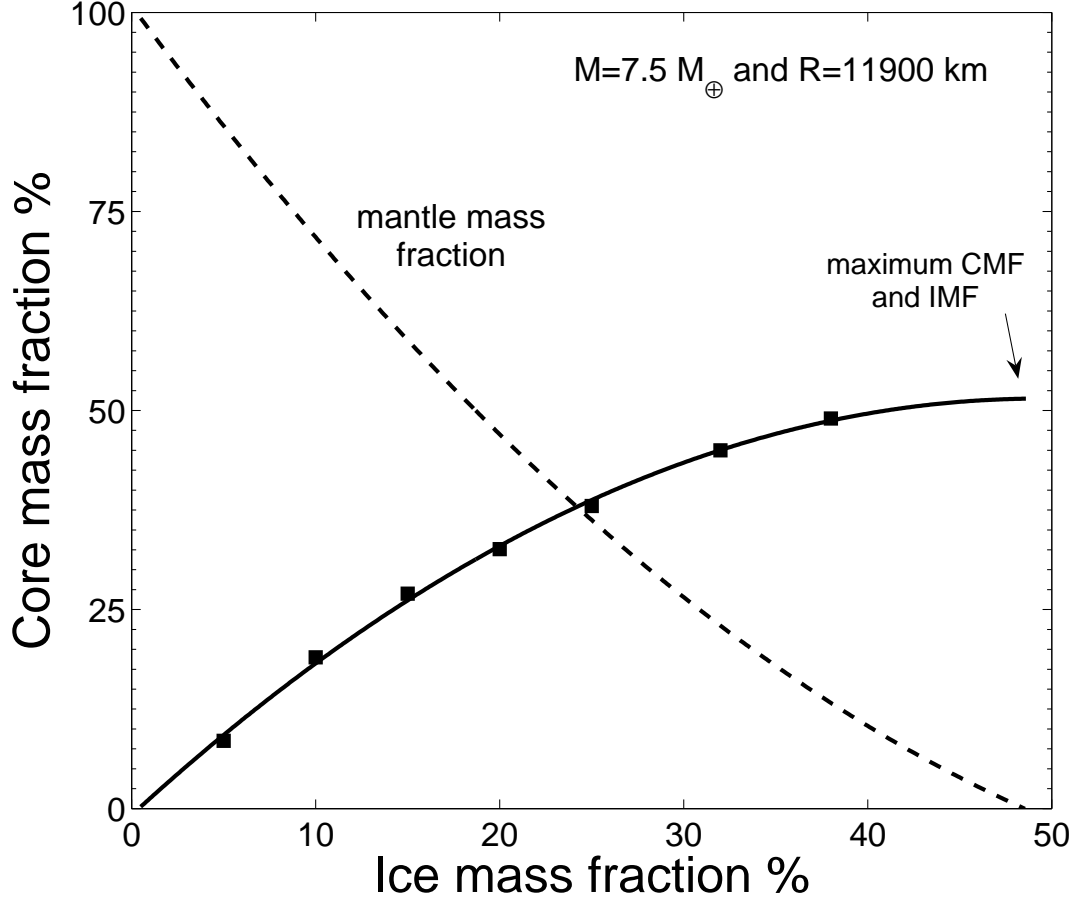


Fig. 4.— Trade-off curve between CMF and IMF. For a planet with $M = 7.5M_{\oplus}$ and $R = 11900$ km the trade-off curve between the amount of ices and amount of mass in the core is depicted as a solid line. The squares correspond to the different data points. The dashed line shows the amount of mass in the mantle. The maximum amount of ices this planet could harbour is 48.6% with CMF=51.4% and no mantle. A planet this size can only be rocky if it had no core (IMF=0 when CMF=0).

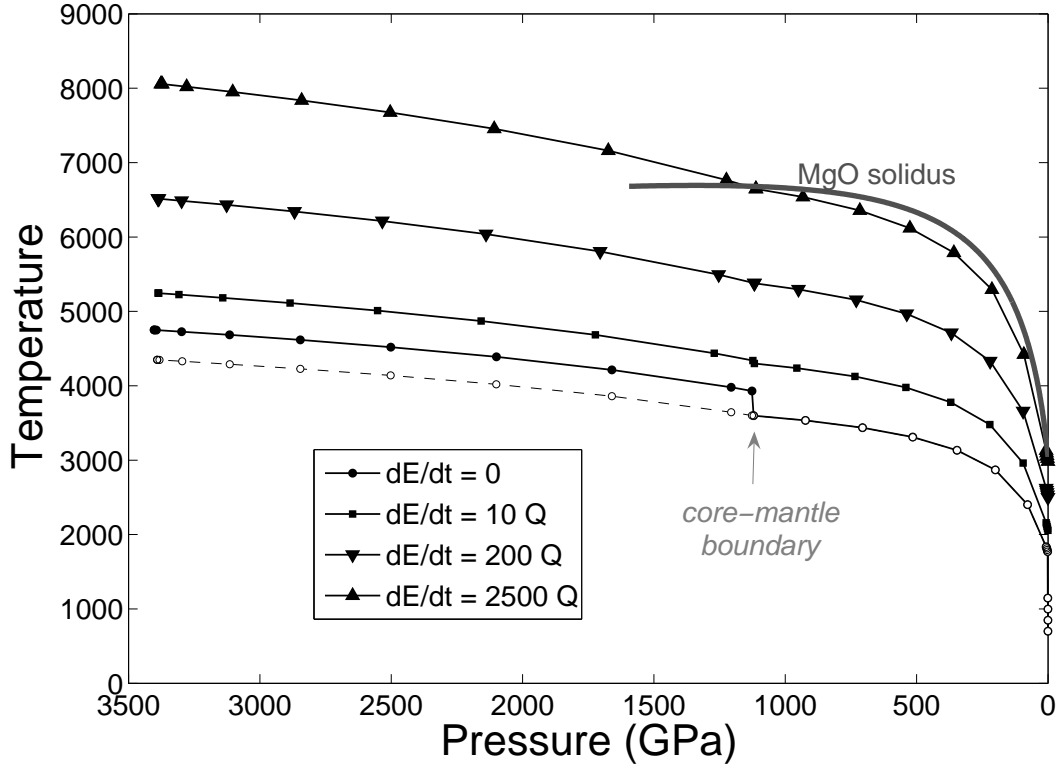


Fig. 5.— Effects of tidal heating on PT structure. PT structure for a $7.5 M_{\oplus}$ planet experiencing different degrees of tidal heating. Dots: no tidal heating. Squares: tidal heating that is 10 times the heat flow without tidal heating (Q) or total heat flow $Q_{total}=3000$ TW. Downward-pointing triangles: 200 times or $Q_{total}=5500$ TW. Upward-pointing triangles: 2500 times or $Q_{total}=68000$ TW. The solidus for MgO is crossed in the mantle when the tidal heating is 2500 times the radioactive and secular cooling contributions. Dotted lines refer to a thermal model without a lower boundary layer in the mantle. As the tidal heating increases the lower boundary layer becomes negligible.